

Graphene–Polypyrrole Nanocomposite as a Highly Efficient and Low Cost Electrically Switched Ion Exchanger for Removing ClO_4^- from Wastewater

Sheng Zhang,^{†,‡} Yuyan Shao,[†] Jun Liu,[†] Ilhan A. Aksay,[§] and Yuehe Lin^{*,†}

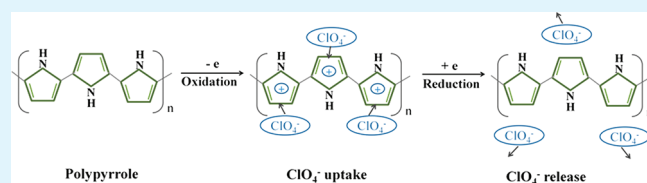
[†]Pacific Northwest National Laboratory, Richland, Washington 99352, United States

[‡]School of Chemical Engineering and Technology, Harbin Institute of Technology, Harbin 150001, China

[§]Department of Chemical and Biological Engineering, Princeton University, Princeton, New Jersey 08544, United States

ABSTRACT: Perchlorate (ClO_4^-) contamination is a widespread concern affecting water utilities. In the present study, functionalized graphene sheets were employed as the scaffold to synthesize a novel graphene–polypyrrole (Ppy) nanocomposite, which served as an excellent electrically switched ion exchanger for perchlorate removal. Scanning electron microscopy and electrochemical measurements showed that the 3D nanostructured graphene–Ppy nanocomposite exhibited a significantly improved uptake capacity for ClO_4^- compared with Ppy film alone. X-ray photoelectron spectroscopy confirmed the uptake and release process of ClO_4^- in graphene–Ppy nanocomposite. In addition, the presence of graphene substrate resulted in high stability of graphene–Ppy nanocomposite during potential cycling. The present work provides a promising method for large scale water treatment.

KEYWORDS: graphene, polypyrrole, perchlorate, uptake capacity, ion exchange, water treatment



1. INTRODUCTION

Perchlorate (ClO_4^-) is a critical component in combat munitions, rocket fuels, and fireworks.¹ There is a significant health concern since ClO_4^- can block the uptake of iodine in the thyroid gland and affect the production of the thyroid hormones.^{2,3} However, due to its high solubility and nonreactivity, ClO_4^- can exist in water for many decades. Therefore, ClO_4^- contamination is now recognized as a widespread concern affecting water utilities. It is difficult to remove ClO_4^- using the conventional separation technology.^{4,5} Recently, an electrically switched ion exchange (ESIX) system has been developed as a green separation technology for removing ClO_4^- and Cs^+ ions from wastewater,^{2,6–9} where the uptake and release of ions is controlled directly by the applied potential.

Conducting polymers have attracted considerable attention due to the promising applications in energy storage/conversion, optoelectronics, chemical sensors, and separations.^{9–11} Among the conducting polymers, polypyrrole (Ppy) and its derivatives have attracted considerable attention because of their stability and potential use as an excellent ion exchange material to selectively remove the ClO_4^- ions in water.^{2,9} The ClO_4^- ion uptake occurs during electrochemical oxidation of Ppy by applying an anodic potential which forces ClO_4^- from the waste solution into the film. The ClO_4^- release occurs when the potential is switched to cathode, forcing ClO_4^- out of the film into the elution solution. The Ppy-based ESIX system can be repeatedly used to significantly reduce the secondary waste. However, its disadvantage is the limited capacity and the poor stability for the removal of ClO_4^- ions. One possible approach is to employ a substrate² which can provide many nucleation sites

for the deposition of Ppy and also act as a substrate to prevent Ppy film from structural destruction.

Graphene, a single-atom-thick carbon material with large surface area, superior chemical stability, and low production cost,^{12–14} could act as an ideal substrate for depositing functional materials for high-performance electrocatalytic or electrochemical devices.^{15–19} The graphene–Ppy nanocomposites have been synthesized and used as electrochemical sensors and supercapacitors.^{20–22} In this report, to the best of our knowledge, we demonstrate the first use of graphene–Ppy nanocomposite in water purification. The graphene–Ppy nanocomposite was prepared by an electrochemical method using functionalized graphene sheets (FGSs) that can be produced in bulk quantities,^{23,24} which was characterized and evaluated as a superior electrically switched ion exchanger for removing ClO_4^- ions. This makes it more practical to use a low cost graphene-based composite for large scale water treatment.

2. EXPERIMENTAL SECTION

Functionalized graphene sheet used in this study was prepared through a thermal expansion process which yields a functionalized (with epoxy and hydroxyl groups) and a defective form of graphene.²³ This functionalized graphene (referred to as graphene in the rest of the paper) was dispersed in ethanol with the aid of ultrasonication. The graphene suspension ($10 \mu\text{L}$, 2 mg mL^{-1}) was applied onto prepolished glassy carbon (GC) working electrode (5 mm in diameter) and dried at room temperature. The graphene–Ppy nanocomposite was prepared by

Received: June 28, 2011

Accepted: August 4, 2011

Published: August 04, 2011

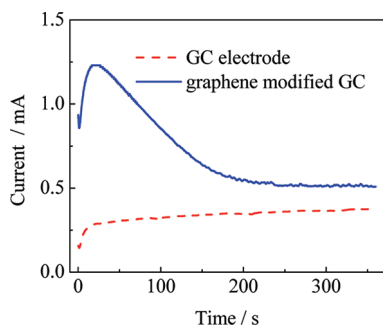


Figure 1. Amperometric $i-t$ curves for electrodeposit of Ppy films on the GC electrode and graphene modified GC electrode.

electrochemical polymerization of polypyrrole on the graphene sheets, which was carried out in a standard three-electrode system controlled CHI660C station with Pt wire and Ag/AgCl as the counter and reference electrodes, respectively. The Ppy film was deposited on graphene modified GC electrode by a constant potential of 0.7 V vs. Ag/AgCl for a period of 6 min in an N_2 -purged aqueous solution containing 0.125 M pyrrole monomer and 0.2 M NaCl. For comparison, the Ppy film on the bare GC electrode was synthesized via the same method. After electropolymerization, the modified working electrode was completely rinsed with deionized water.

Scanning electron microscopy (SEM) images were obtained with an FEI Helios Nanolab dual-beam focused ion beam/scanning electron microscope (FIB/SEM) operated at 2 kV. X-ray photoelectron spectroscopy (XPS) measurements were made using a Physical Electronics Quantum-5600 Scanning ESCA Microprobe. Al X-ray source was operated at 250 W. The sample to analyzer takeoff angle was 45° . Survey spectra were collected at a pass energy (PE) of 187.85 eV over the binding energy range of 0–1300 eV. High binding energy resolution Multiplex data for the individual elements were collected at a PE of 29.55 eV.

3. RESULTS AND DISCUSSION

The amperometric $i-t$ curves during the electrochemical deposition of polypyrrole at the bare GC electrode and the graphene modified GC electrode are shown in Figure 1. In contrast to the case of GC electrode, a distinct current peak within the first seconds is observed for the graphene modified GC electrode. This suggests different nucleation processes in the initial stages of Ppy electropolymerization:²⁵ most likely, a higher number of nucleation sites is generated on graphene modified GC electrode compared to the bare GC electrode which can be attributed to the high surface area and electronic conductivity of graphene nanosheets.²⁶ The SEM image in Figure 2A shows the graphene sheets of a few micrometers in lateral size with the characteristic lamellar structure of graphene.²⁷ Figure 2B,C shows typical Ppy nanostructures containing spherical particles with diameters ranging from 200 to 800 nm for both Ppy and graphene–Ppy. However, Ppy film on GC electrode (Figure 2B) is very compact and lacks nanoporosity, while the Ppy film in graphene–Ppy nanocomposite (Figure 2C) is loose and contains many spherical particles creating a 3D porous nanostructure which can be highly beneficial for ion diffusion.²⁸ Commensurate with these characteristics, below, we demonstrate that the graphene–Ppy nanocomposites indeed exhibit a high performance for the removal of ClO_4^- ions.

The electroactivity and the reversible redox properties of Ppy have attracted great interest in the development of electrochemically

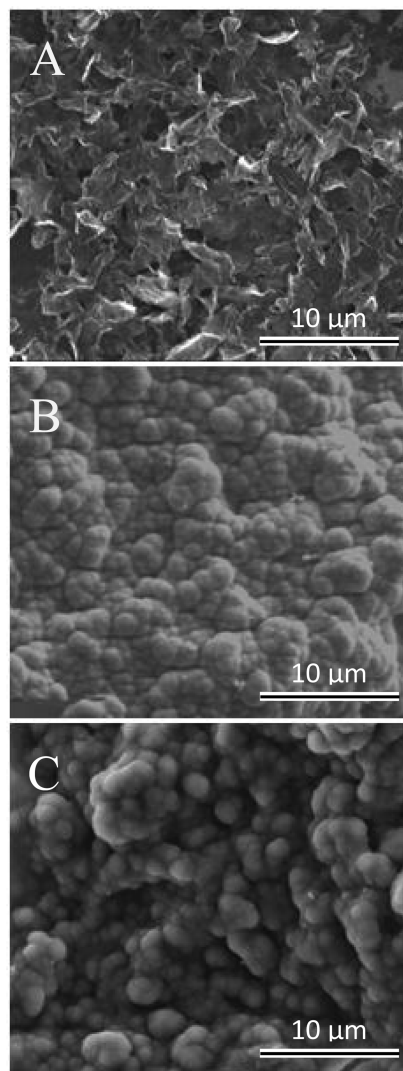


Figure 2. SEM images of graphene (A), Ppy (B), and graphene–Ppy (C).

controlled delivery devices and separation systems for charged species.^{29,30} When Ppy films are cycled in appropriate electrolytes, the reversible redox switching of the film is accompanied by the movement of counterions in and out of the polymer film for charge balance. Figure 3 shows the schematic illustration of the electrically controlled anion exchange for the separation of the perchlorate ion from wastewaters using Ppy film as the electroactive ion exchanger. The ClO_4^- ion uptake occurs when the electrochemical oxidation of the electroactive species is performed by applying an anodic potential on the film in the solution containing ClO_4^- which forces the ClO_4^- from the waste solution into the film. Correspondingly, the ClO_4^- ion release occurs when the potential is switched to cathode which forces the ClO_4^- out of the film and into the elution solution. To maintain the charge balance, the charges during the oxidation and reduction of Ppy films are compensated with the same amount of ClO_4^- into and out of Ppy films.

Cyclic voltammetry is a useful tool to evaluate the capacity of electroactive materials. Figure 4 shows the cyclic voltammograms (CVs) of graphene, Ppy film, and graphene–Ppy films in 0.2 M $NaClO_4$ solution. The CV on graphene shows the rectangular and symmetric current–potential characteristics, and there are

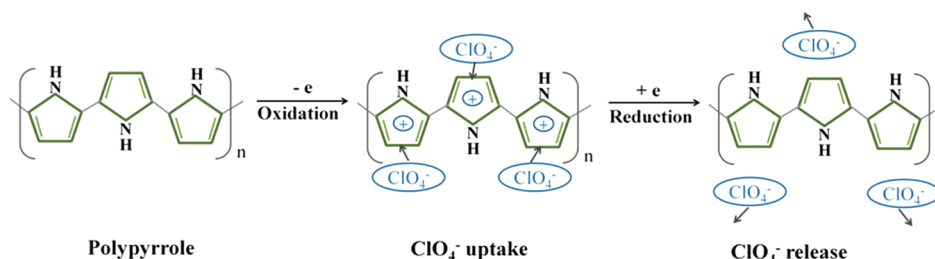


Figure 3. Schematic illustration for the uptake and release process of ClO_4^- with the oxidation and reduction of Ppy films.

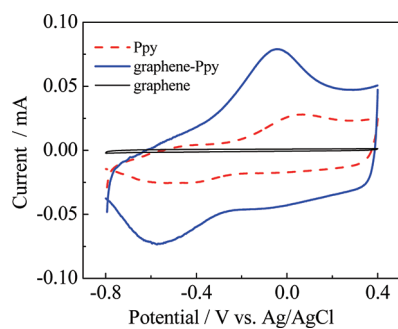


Figure 4. Cyclic voltammograms (2 mV s^{-1}) of Ppy and graphene–Ppy films in 0.2 M NaClO_4 solution.

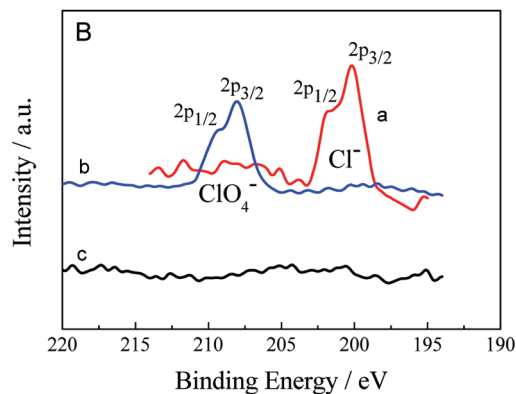
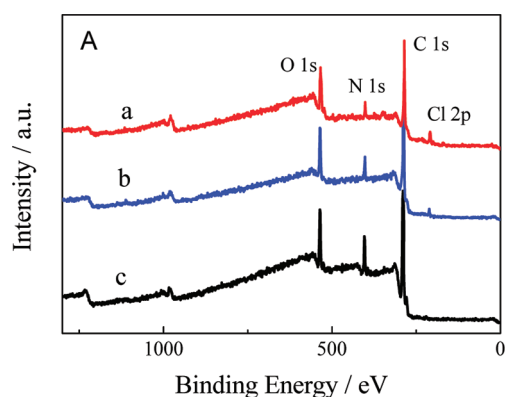


Figure 6. XPS survey (A) and high resolution Cl spectrum (B) of as-prepared graphene–Ppy nanocomposite (a) and after controlling the electrode at 0.4 V for 600 s (b) and at -0.8 V for 600 s (c) in a solution containing 0.2 M NaClO_4 .

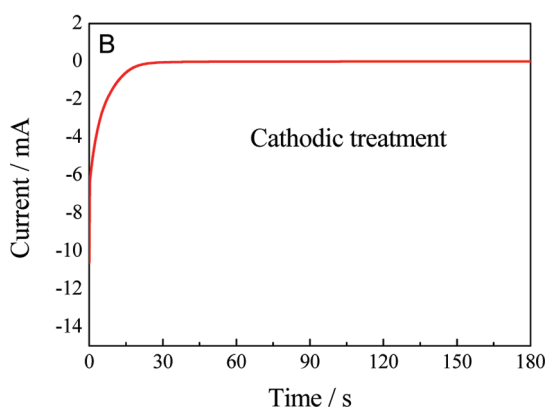
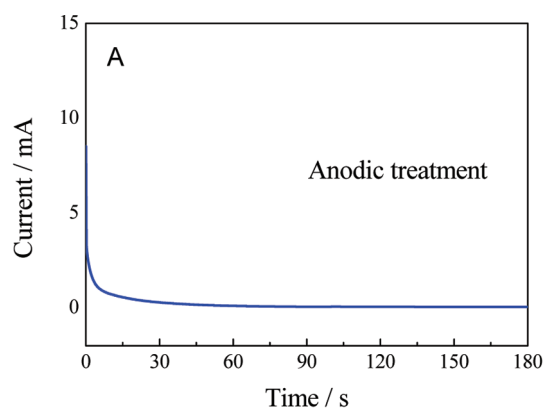


Figure 5. $i-t$ curve during the anodic (0.4 V) and cathodic (-0.8 V) treatment in 0.2 M NaClO_4 solution.

no clear redox peaks observed in the potential range between -0.8 and $+0.4 \text{ V}$. However, a relatively sharp oxidation peak and a

broad reduction peak are observed on both Ppy and graphene–Ppy films which are characteristic of Ppy films.^{31,32} The ion uptake and release can be controlled by modulating the electrode potential: during the oxidation, cationic sites such as polarons (Ppy^+) are formed on the Ppy film, and at the same time, the anion species such as ClO_4^- in the solution are forced into the Ppy film to balance the positive charges; correspondingly, the ClO_4^- ions are released from Ppy film during the reduction process. A much higher oxidation peak current can be observed on the graphene–Ppy film which is 2.5 times higher than that of the Ppy film. It is obvious that the charges during the oxidation of graphene–Ppy film are much higher than that of the Ppy film. These charges during the Ppy oxidation are compensated with the same amount of ClO_4^- ions into the Ppy film or graphene–Ppy film. We, therefore, conclude that the graphene–Ppy film has a much higher uptake capacity for ClO_4^- than the Ppy film. The possible reason for this

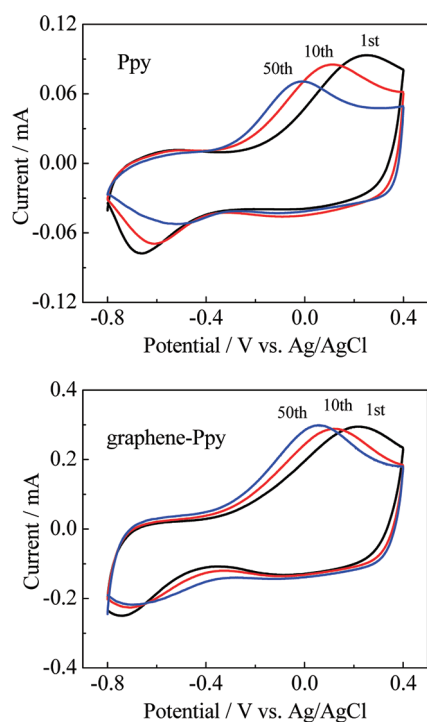


Figure 7. Consecutive cyclic voltammograms for Ppy and graphene-Ppy films in 0.2 M NaClO₄ solution. The scan rate: 5 mV s⁻¹.

higher uptake is that the 3D porous nanostructure of the graphene-Ppy film facilitates ClO₄⁻ to easily diffuse into or out of the film.

The process of electrically switched anion exchange for ClO₄⁻ ions may proceed at a higher rate. The *i*-*t* curves in Figure 5, recorded during the anodic and cathodic treatment for graphene-Ppy film, exhibited that the process of electrically switched anion exchange almost finished within 20 s. XPS was employed to provide further evidence for the uptake and the release process of ClO₄⁻ in graphene-Ppy nanocomposite. Figure 6 shows the XPS spectrum of the as-prepared graphene-Ppy nanocomposite (line a) and after different electrochemical treatments (lines b and c). As shown in Figure 6A(a),B(a), the appearance of peaks around 200 eV indicates that Cl⁻ was doped into Ppy film in graphene-Ppy nanocomposite during the polymerization. Figure 6A(b),B(b) shows the XPS data of graphene-Ppy nanocomposite after an applied anodic potential of 0.4 V for 600 s in a solution containing 0.2 M NaClO₄. The peaks around 210 eV can be distinguished which means that the ClO₄⁻ has been taken into the Ppy film in the graphene-Ppy nanocomposite under an anodic potential. Then, the graphene-Ppy nanocomposite was cathodically polarized at -0.8 V for 600 s in a solution of 0.2 M NaClO₄. As shown in Figure 6A(c),B(c), the peaks of Cl 2p disappeared, indicating that almost all the ClO₄⁻ anions were ejected out of the film which reflects the feasibility of electrically controlled anion exchange. The Cl⁻ ion is spherical with a radius of 0.181 nm, while the shape of ClO₄⁻ is tetrahedral with a size of 0.240 nm. These differences in shape and size will exert an influence on their strength of interaction with Ppy chains and also on their mobility in and out of the Ppy films. Studies confirmed that the mobility of ClO₄⁻ was smaller than that of Cl⁻, which results in the preferential ClO₄⁻ selectivity over Cl⁻ for Ppy film.²

The stability of Ppy film is one of the key factors for its application as an ion exchanger. The consecutive CVs shown in Figure 7 indicate that the loss of capacity for ClO₄⁻ exchange occurs quickly on repeated cycling for the Ppy film on the bare GC electrode. In contrast, the oxidation peak current on graphene-Ppy film keeps constant during the consecutive cycling. In addition, the oxidation peaks gradually shift negatively for both Ppy and graphene-Ppy films which is due to the structural relaxation of Ppy film with potential cycling.² The negative shift of the peak potential on the graphene-Ppy film is much smaller than that on the Ppy film, indicating less structural change on the graphene-Ppy film. These results indicate that the stability of the Ppy film is significantly improved when it is deposited on the surface of graphene which can be attributed to the possibility that the large particle-sized graphene substrate prevents the structural change of Ppy film.

4. CONCLUSIONS

Functionalized graphene-polypyrrole nanocomposites were processed using an electrodeposition method. The nanocomposite improved the capacity for ClO₄⁻ exchange which we attribute to its 3D porous nanostructure facilitating an easy ClO₄⁻ diffusion into or out of the Ppy film. Further, the presence of graphene substrate resulted in an improved stability of Ppy film during potential cycling. Therefore, our present study provides a green process for removing ClO₄⁻ from wastewater through an electrically switched ion exchange. Moreover, this novel graphene-Ppy film may find applications in other fields, such as supercapacitors and chemical sensors.

AUTHOR INFORMATION

Corresponding Author

*E-mail: yuehe.lin@pnl.gov.

ACKNOWLEDGMENT

The work was done at Pacific Northwest National Laboratory (PNNL) and was supported by the U.S. Department of Defense's SERDP environmental research program (Project ER-1433). The characterization was performed using Environmental Molecular Sciences Laboratory, a national scientific-user facility sponsored by the DOE's Office of Biological and Environmental Research and located at PNNL. PNNL is operated for DOE by Battelle under Contract DE-AC05-76RL01830. The authors would like to acknowledge Dr. Laxmikant Saraf for SEM measurement. S.Z. acknowledges a fellowship from the China Scholarship Council and PNNL to perform this work at PNNL.

REFERENCES

- Urbansky, E. *Environ. Sci. Pollut. Res.* **2002**, *9*, 187–192.
- Lin, Y. H.; Cui, X. L.; Bontha, J. *Environ. Sci. Technol.* **2006**, *40*, 4004–4009.
- Crump, K. S.; Gibbs, J. P. *Environ. Health Perspect.* **2005**, *113*, 1001–1008.
- Gu, B. H.; Ku, Y. K.; Brown, G. M. *Environ. Sci. Technol.* **2005**, *39*, 901–907.
- Almeida, C.; Giannetti, B. F.; Rabockai, T. *J. Electroanal. Chem.* **1997**, *422*, 185–189.
- Lin, Y. H.; Cui, X. L. *Chem. Commun.* **2005**, 2226–2228.
- Cui, X. L.; Engelgard, M. H.; Lin, Y. H. *J. Nanosci. Nanotech.* **2006**, *6*, 547–553.

- (8) (a) Lin, Y. H.; Cui, X. L. *J. Mater. Chem.* **2006**, *16*, 585–592.
(b) Chen, W.; Xia, X. H. *Adv. Funct. Mater.* **2007**, *17*, 2943–2948.
- (9) (a) Lin, Y. H.; Choi, D.; Wang, J.; Bontha, J.R. Nanomaterials-Enhanced Electrically Switched Ion Exchange Process for Water Treatment. In *Nanotechnology Applications for Clean Water*; Diallo, M.; Duncan, J.; Savage, N.; Street, A.; Sustich, R., Eds.; William Andrew: Norwich, NY, 2009, Chapter 14, pp 179–189. (b) Wu, J. C.; Mullett, W. M.; Pawliszyn, J. *Anal. Chem.* **2002**, *74*, 4855–4859.
- (10) Wang, J.; Chan, S.; Carlson, R. R.; Luo, Y.; Ge, G. L.; Ries, R. S.; Heath, J. R.; Tseng, H. R. *Nano Lett.* **2004**, *4*, 1693–1697.
- (11) Zhang, D.; Zhang, X.; Chen, Y.; Yu, P.; Wang, C.; Ma, Y. *J. Power Sources* **2011**, *196*, 5990–5996.
- (12) Tang, L. H.; Wang, Y.; Li, Y. M.; Feng, H. B.; Lu, J.; Li, J. H. *Adv. Funct. Mater.* **2009**, *19*, 2782–2789.
- (13) Zhang, S.; Shao, Y. Y.; Liao, H. G.; Liu, J.; Aksay, I. A.; Yin, G. P.; Lin, Y. H. *Chem. Mater.* **2011**, *23*, 1079–1081.
- (14) Qu, L. T.; Liu, Y.; Baek, J. B.; Dai, L. M. *ACS Nano* **2010**, *4*, 1321–1326.
- (15) Murugan, A. V.; Muraliganth, T.; Manthiram, A. *Chem. Mater.* **2009**, *21*, 5004–5006.
- (16) Shao, Y. Y.; Zhang, S.; Engelhard, M. H.; Li, G. S.; Shao, G. C.; Wang, Y.; Liu, J.; Aksay, I. A.; Lin, Y. H. *J. Mater. Chem.* **2010**, *20*, 7491–7496.
- (17) Meng, X. B.; Geng, D. S.; Liu, J. A.; Banis, M. N.; Zhang, Y.; Li, R. Y.; Sun, X. L. *J. Phys. Chem. C* **2010**, *114*, 18330–18337.
- (18) Wang, D. W.; Gentle, I. R.; Lu, G. Q. *Electrochem. Commun.* **2010**, *12*, 1423–1427.
- (19) Shao, Y. Y.; Zhang, S.; Wang, C. M.; Nie, Z. M.; Liu, J.; Wang, Y.; Lin, Y. H. *J. Power Sources* **2010**, *195*, 4600–4605.
- (20) Liu, A. R.; Li, C.; Bai, H.; Shi, G. Q. *J. Phys. Chem. C* **2010**, *114*, 22783–22789.
- (21) Scott, C. L.; Zhao, G. J.; Pumera, M. *Electrochem. Commun.* **2010**, *12*, 1788–1791.
- (22) Bose, S.; Kuila, T.; Uddin, M. E.; Kim, N. H.; Lau, A. K. T.; Lee, J. H. *Polymer* **2010**, *51*, 5921–5928.
- (23) Schniepp, H. C.; Li, J. L.; McAllister, M. J.; Sai, H.; Herrera-Alonso, M.; Adamson, D. H.; Prud'homme, R. K.; Car, R.; Saville, D. A.; Aksay, I. A. *J. Phys. Chem. B* **2006**, *110*, 8535–8539.
- (24) McAllister, M. J.; Li, J. L.; Adamson, D. H.; Schniepp, H. C.; Abdala, A. A.; Liu, J.; Herrera-Alonso, M.; Milius, D. L.; Car, R.; Prud'homme, R. K.; Aksay, I. A. *Chem. Mater.* **2007**, *19*, 4396–4404.
- (25) Earley, S. T.; Dowling, D. P.; Lowry, J. P.; Breslin, C. B. *Synth. Met.* **2005**, *148*, 111–118.
- (26) Wang, D. W.; Li, F.; Zhao, J. P.; Ren, W. C.; Chen, Z. G.; Tan, J.; Wu, Z. S.; Gentle, I.; Lu, G. Q.; Cheng, H. M. *ACS Nano* **2009**, *3*, 1745–1752.
- (27) Zhang, S.; Shao, Y.; Liao, H.; Engelhard, M. H.; Yin, G.; Lin, Y. *ACS Nano* **2011**, *5*, 1785–1791.
- (28) Jung, Y. J.; Singh, N.; Choi, K. S. *Angew. Chem., Int. Ed.* **2009**, *48*, 8331–8334.
- (29) Wu, J.; Mullett, W. M.; Pawliszyn, J. *Anal. Chem.* **2002**, *74*, 4855–4859.
- (30) Johanson, U.; Marandi, M.; Tamm, T.; Tamm, J. *Electrochim. Acta* **2005**, *50*, 1523–1528.
- (31) Dione, G.; Dieng, M. M.; Aaron, J. J.; Cachet, H.; Cachet, C. *J. Power Sources* **2007**, *170*, 441–449.
- (32) Hughes, M.; Chen, G. Z.; Shaffer, M. S. P.; Fray, D. J.; Windle, A. H. *Chem. Mater.* **2002**, *14*, 1610–1613.